Chinese Physics Letters

LETTER

Condensate Fraction Scaling and Berezinskii−Kosterlitz−Thouless Transition of Superconductivity and Superfluidity

Cite as: Yuan-Yao He. 2026 *Chin. Phys. Lett.* **43** 080703

DOI CSTR

Recommended Articles

Evolution of Superconducting-Transition Temperature with Superfluid Density and Conductivity in Pressurized Cuprate Superconductors
Jinyu Zhao *et al*.
Chin. Phys. Lett. **41**, (2024)

Phase coherence of charge-6*e* superconductors with a frustrated Kagome XY antiferromagnet
Feng-Feng Song, and Guang-Ming Zhang
Chin. Phys. Lett. **42**, 037401 (2025)

Complete Universal Scaling in First-Order Phase Transitions
Fan Zhong
Chin. Phys. Lett. **41**, 100502 (2024)

Two-Dimensional XY Ferromagnet Induced by Long-Range Interaction
Tianning Xiao, Dingyun Yao, Chao Zhang, Zhijie Fan, and Youjin Deng
Chin. Phys. Lett. **42**, 070002 (2025)

Is There Kibble-Zurek Scaling of Topological Defects in First-Order Phase Transitions?
Fan Zhong
Chin. Phys. Lett. **42**, 030203 (2025)

Intervalley Band Crossing and Transition of Fractional Chern Insulators in Floquet Twisted Bilayer $MoTe_2$
Yuhao Shi, and Zhao Liu
Chin. Phys. Lett. **43**, 050716 (2026)

A series journal of Chinese Physical Society distributed by IOP Publishing

Chinese Physics Letters

Chin. Phys. Lett. **43** 080703 (2026)

LETTER

DOI: 10.1088/0256-307X/43/8/080703
CSTR: 32039.14.0256-307X.43.8.080703

Condensate Fraction Scaling and Berezinskii–Kosterlitz–Thouless Transition of Superconductivity and Superfluidity

Yuan-Yao He(何院耀)[1,2,3,4,*]

[1]Institute of Modern Physics, Northwest University, Xi'an 710127, China
[2]Shaanxi Key Laboratory for Theoretical Physics Frontiers, Xi'an 710127, China
[3]Fundamental Discipline Research Center for Quantum Science and Technology of Shaanxi Province, Xi'an 710127, China
[4]Hefei National Laboratory, Hefei 230088, China

[*]Corresponding author. Email: heyuanyao@nwu.edu.cn

Characterizing the superconducting and superfluid transitions in two-dimensional (2D) many-body systems is of broad interest and remains a fundamental issue. In this study, we establish the condensate fraction scaling as a highly efficient tool to achieve that and accordingly propose efficient schemes to accurately determine the associated Berezinskii–Kosterlitz–Thouless (BKT) transitions. Using the 2D attractive Fermi-Hubbard model as a testbed and applying numerically exact auxiliary-field quantum Monte Carlo simulations, we access unprecedented system sizes (up to 64 × 64 = 4 096 lattice sites) and perform a comprehensive analysis for the temperature dependence and finite-size scaling of condensate fraction across the BKT transition. We demonstrate that this quantity exhibits algebraic scaling below the transition and exponential scaling above it, with significantly reduced finite-size effects comparing to the extensively studied on-site pairing correlator. This greatly improves the determination of BKT transition using moderate system sizes. We also extract finite-size BKT transition temperature from condensate fraction, and confirm its logarithmic correction on system size. Based on the accurately determined transition, we reveal that the specific heat displays an anomaly, showing a peak at a temperature slightly above BKT transition. Our findings should be generally applicable to 2D fermionic and bosonic systems hosting superconductivity or superfluidity.

Berezinskii–Kosterlitz–Thouless (BKT) transition [1–3] is one of the most intriguing property of two-dimensional (2D) systems with U(1) continuous symmetry and short-range interactions. The transition towards the low-temperature phase is typically characterized [4] by the formation of bounded vortex-antivortex pairs and a quasi-long-range order with algebraically decaying correlation function versus distance. The most representative examples are 2D superconductivity and superfluidity, for which the theory also predicts a universal jump of the superfluid density [5] at the BKT transition. These key signatures of BKT physics was experimentally verified in liquid ^{4}He [6,7] and superconducting films [8–10] soon after the celebrated BKT theory, and more recently in 2D interacting Bose gas [11–13] and Fermi gas [14,15]. The rapid progress in ultracold atom systems has enabled the detailed studies of the BKT transition, and many more experiments with growing precision continue to reveal its other rich properties, such as the phase fluctuations [16], transport and excitation signatures [17–20].

Theoretically, the thorough characterization and precise determination of the BKT transition primarily rely on numerically unbiased calculations [21–43]. Regarding superconductivity and superfluidity, the 2D attractive Hubbard model serves as the minimal model that captures the BKT physics, as investigated by auxiliary-field quantum Monte Carlo (AFQMC) simulations [33–41]. These studies typically estimated the BKT transition temperature through finite-size analyses of the on-site spin-singlet pairing correlation or the superfluid density [44,45]. However, both quantities exhibit pronounced finite-size effects, which compromise the reliability of standard scaling approaches. In addition, extracting superfluid density from the dynamical current-current correlation function is computationally demanding and usually yields notably noisy results [36,38,39]. All of these studies have been constrained to lattice sizes of up to 400 sites, which are likely insufficient to capture the logarithmic finite-size corrections characteristic of BKT transition [23,25,30]. These limitations hinder high-precision determination of BKT transition temperature, even when using numerically exact AFQMC simulations.

Alternatively, condensate fraction is also a fundamental quantity to characterize the superconducting and superfluid states [46–48], defined as the proportion of Bose-condensed bosons or fermion pairs. It was experimentally measured in liquid ^{4}He [49] system and ultracold Fermi gas [50–52] in three dimensions, and found to behave similarly as the pairing order parameter with its onset identifying the superfluid phase transtion. In these systems, this quantity has also been theoretically computed by mean-field theories [48,53–55] as well as many-body numerical methods [47,56–59] at both ground state and finite temperatures. In contrast, it is much less studied for 2D superconductivity and superfluidity in many-body systems especially at finite temperatures. Until now, the theoretical and numerical studies of this quantity mainly concentrate on the ground-state results of 2D interacting Fermi gas [60–62]. Then the natural questions arise as the behaviors of this quantity around the BKT transition and whether it could be used to probe the transition.

We address the questions by systematically exploring the temperature and size dependences of condensate fraction across the BKT transition in the 2D attractive Hubbard model with large-scale and numerically unbiased AFQMC algorithm. Our calculations reach lattice sizes of up to 4096 sites, an order of magnitude larger than that in previous studies [33–41]. This enables us to perform a finite-size scaling analysis of BKT physics in correlated fermion systems with unprecedented high quality. Our numerical results reveal the algebraic (exponential) scaling of condensate fraction in the superfluid (normal) phase, and establish it as a much more effective probe for characterizing the BKT transition, compared to the long-studied on-site pairing correlator. Then we have computed accurate BKT transition temperature based on the scaling behaviors of condensate fraction. A clear evidence of specific heat anomaly above the BKT transition is also identified in our calculations.

Received 19 May 2026; accepted 30 June 2026; published 22 July 2026
© 2026 Chinese Physical Society and IOP Publishing Ltd. All rights, including for text and data mining, AI training, and similar technologies, are reserved.

Check for updates

We study the 2D attractive Fermi-Hubbard model on square lattice with the Hamiltonian as

$$\hat{H} = \sum_{k\sigma}(\varepsilon_{\boldsymbol{k}} + \mu)c^{+}_{k\sigma}c_{k\sigma} + U\sum_{i}\left(\hat{n}_{i\uparrow}\hat{n}_{i\downarrow} - \frac{\hat{n}_{i\uparrow}+\hat{n}_{i\downarrow}}{2}\right),$$

with $\hat{n}_{i\sigma} = c^{+}_{i\sigma}c_{i\sigma}$ as the density operator and σ (=↑ or ↓) denoting spin. We only consider the nearest-neighbor hopping t with the energy dispersion $\varepsilon_{\boldsymbol{k}} = -2t(\cos k_x + \cos k_y)$, where k_x, k_y are the momentum defined in units of $2\pi/L$ with linear system size L. The fermion filling is $n = N_e/N_s$ with $N_s = L^2$ and N_e as the number of lattice sites and fermions. We set t as the energy unit, and focus on attractive interaction $U < 0$ with hole doping $\mu > 0$. It is well-known that this model has a superconducting ground state [63–65] and exhibits BKT transition at finite temperatures [33–36]. We employ state-of-art AFQMC algorithm [66–72] with most recent developments [see the Supplemental Material (SM) for details] to study the BKT physics in this model. Our simulations cover a large range of system sizes, from $L = 8$ to $L = 64$.

We mainly focus on the condensate fraction and on-site pairing correlator, which both characterize the fermion pairing. The first is initially defined from the macroscopic eigenvalue of the two-body density matrix, expressed as $\boldsymbol{\rho}(\boldsymbol{r},\boldsymbol{r}') = \{\langle c^{+}_{i\uparrow}c^{+}_{j\downarrow}c_{i+r\uparrow}c_{j+r'\downarrow}\rangle\}$, in asymptotic limit $|\boldsymbol{r}|,|\boldsymbol{r}'| \to \infty$ [46,47]. Regarding attractive interaction, we only need to focus on the dominant component of $\boldsymbol{\rho}(\boldsymbol{r},\boldsymbol{r}')$, i.e., the pairing matrix in momentum space [42,43,61] as $M_{\boldsymbol{k}\boldsymbol{k}'} = \langle\hat{\Delta}^{+}_{\boldsymbol{k}}\hat{\Delta}_{\boldsymbol{k}'}\rangle - \delta_{\boldsymbol{k}\boldsymbol{k}'}\langle c^{+}_{\boldsymbol{k}\uparrow}c_{\boldsymbol{k}\uparrow}\rangle\langle c^{+}_{-\boldsymbol{k}\downarrow}c_{-\boldsymbol{k}\downarrow}\rangle$, with $\hat{\Delta}^{+}_{\boldsymbol{k}} = c^{+}_{\boldsymbol{k}\uparrow}c^{+}_{-\boldsymbol{k}\downarrow}$ as the $\boldsymbol{k}$-space spin-singlet pairing operator. Then condensate fraction can be calculated as $n_c = \lambda_{\max}/(N/2)$, with $\lambda_{\max}$ as the leading eigenvalue of $M_{\boldsymbol{k}\boldsymbol{k}'}$ matrix. The corresponding eigenvector of $\lambda_{\max}$ contains the pairing structure information in $\boldsymbol{k}$ space (see the SM for details). On the other hand, the pairing correlation function is defined as $P(\boldsymbol{r}) = L^{-2}\sum_i\langle\hat{\Delta}^{+}_{i}\hat{\Delta}_{i+\boldsymbol{r}} + \hat{\Delta}_{i}\hat{\Delta}^{+}_{i+\boldsymbol{r}}\rangle/4$ with the on-site pairing operator $\hat{\Delta}^{+}_{i} = c^{+}_{i\uparrow}c^{+}_{i\downarrow}$. The corresponding pairing correlator reads $\langle\Delta^2\rangle = L^{-2}\sum_{\boldsymbol{r}}P(\boldsymbol{r})$, which has been studied for attractive fermions over decades [33–41]. For 2D superfluid phase, $P(\boldsymbol{r})$ decays algebraically as $P(\boldsymbol{r}) \propto r^{-\eta}$ with $\eta \leqslant \eta_c$ and $\eta_c = 1/4$ at BKT transition [1–3], leading to the scaling behavior of $\langle\Delta^2\rangle \propto L^{-\eta}$ in large L limit (see the SM for details). In contrast, they simply decay exponentially in the normal phase.

As the main results of this work, figure 1 summarizes finite-size scaling behaviors of condensate fraction n_c and on-site pairing correlator $\langle\Delta^2\rangle$ for $U/t = -4, \mu/t = 0.25$. Upon cooling, n_c monotonically grows as evolving from the normal phase to the superfluid phase (see the SM for details). Then the log-log plot and fittings for the numerical results in Fig. 1(a) clearly reveal that n_c also has algebraic ($\propto L^{-\eta}$) and exponential ($\propto \exp(-\alpha L)$) scalings versus L in the low and high temperature regimes, respectively. As a comparison, Fig. 1(b) plots $\langle\Delta^2\rangle L^{1/4}$ versus L, and the results with $L \geqslant 32$ confirm the size-scaling behaviors of $\langle\Delta^2\rangle$ from BKT theory. As it is straightforward, the horizontal line (gray, dash-dot) denoting $\eta_c = 1/4$ in Fig. 1(b) determines the BKT transition temperature in the range of 0.140–0.145, which perfectly matches to that from n_c results in Fig. 1(a). Moreover, the fittings of these two quantities presents well consistent exponents $\eta(T)$ within statistical uncertainty, indicating exactly the same size-scaling behavior of them (in large L limit). Note that at $T/t = 0.145$, the algebraic scaling should gradually cross over to exponential decay at larger system sizes even beyond the reach of our AFQMC calculations. These results explicitly illustrate the vanishing n_c and $\langle\Delta^2\rangle$ approaching the thermodynamic limit (TDL) at finite temperatures, thereby confirming the quasi-condensate and quasi-long-range order state in the 2D superfluid phase. Furthermore, the exponent $\eta(T)$ exhibits a linear dependence on T as $T \to T^{-}_{\mathrm{BKT}}$ [5]. We accordingly perform a linear extrapolation for $\eta(T)$ to the critical η_c, and reach the transition temperature $T_{\mathrm{BKT}}/t = 0.1420(7)$ at TDL, as shown in the inset of Fig. 1(a).

It is notable that Fig. 1 reveals a prominent discrepancy between n_c and $\langle\Delta^2\rangle$. The former already reaches the scaling regime for $L \geqslant 20$, whereas the latter exhibits the correct asymptotic behavior only for $L \geqslant 32$. $\langle\Delta^2\rangle$ shows pronounced finite-size effects, with results for $L < 32$ clearly deviating from the asymptotic scaling observed in larger systems, as shown in Fig. 1(b). If the numerical simulations are restricted to $L = 20$, as in previous studies [33,34,36–41], one would obtain the BKT transition temperature in the range $0.12 < T_{\mathrm{BKT}}/t < 0.13$, consistent with that reported in Ref. [41], but with an error exceeding 10% relative to the correct value. Nevertheless, condensate fraction n_c shown in Fig. 1(a) exhibits much better size-scaling behavior around BKT transition. Results within $L \leqslant 20$ can determine the BKT transition temperature, with a small interval of $0.005\,t$, pinning it down to the quantitatively correct range. These results demonstrate that the condensate fraction exhibits significantly weaker finite-size effects, reaching the asymptotic scaling regime at much smaller system sizes than the on-site pairing correlator. This distinction is crucial for practical numerical studies, where accessible system sizes are limited, as the condensate fraction converges much more rapidly to the asymptotic behavior.

The above scaling difference can be attributed to the distinct underlying physics of these two quantities. Formally, $\langle\Delta^2\rangle$ includes a subleading correction $\propto L^{-2}$ (see the SM for details), in addition to the leading term $\propto L^{-\eta}$. Physically, while $\langle\Delta^2\rangle$ only accounts for on-site pairing, the pairing matrix $M_{\boldsymbol{k}\boldsymbol{k}'}$ originates from $\boldsymbol{k}$-space pairing, meaning that n_c encompasses contributions from Cooper pairs of all possible sizes. For weak to intermediate attractive interactions, nonlocal fermion pairing is non-negligible, as evidenced by AFQMC results of real-space pair wave function (see the SM for details), and has also been observed in a recent optical lattice experiment [73]. The contribution from local Cooper pairs to the overall pairing can fluctuate significantly with system size. Consequently, the quantity $\langle\Delta^2\rangle$ fails to capture the full pairing structure of the system and it is subject to strong finite-size effects regarding the asymptotic scaling (i.e., $\langle\Delta^2\rangle \propto L^{-\eta}$).

We have obtained similar results as Fig. 1 for different U/t and μ/t, and have verified the same scaling behaviors in fixed-μ and fixed-density calculations (see the SM for details). We present fixed-μ results to enable efficient access to large system sizes within the grand-canonical framework, since achieving fixed density requires iterative tuning of μ, which becomes increasingly costly for large L. This consideration is particularly relevant here. The on-site pairing correlator has strong finite-size effects and needs $L \geqslant 32$ to reach the correct scaling regime, making fixed-density calculations much more demanding. In contrast, the condensate fraction yields reliable estimates already at moderate system sizes within the same framework.

Our numerical results show that, the finite-size effect of the on-site pairing correlator $\langle\Delta^2\rangle$, manifested as deviation from the correct scaling in small sizes, gets more severe at lower filling and weaker interaction. This can be understood from the fact that the nonlocal pairing becomes more significant in these systems. Instead, such effect is almost absent in condensate fraction n_c with its numerical results always exhibiting nice size-scaling behavior for $L \geqslant 12$ as those shown in Fig. 1(a). This indicates that accurately determining the BKT transition in 2D interacting Fermi gas [43] via finite-size analysis of $\langle\Delta^2\rangle$ is considerably more challenging than using n_c. All these results suggest that condensate fraction is a more appropriate quantity for characterizing the fermion pairing and determining BKT transition for attracive fermions. Our calculations of superfluid density [44,45] up to $L = 32$ also agree with the BKT transition temperature obtained from the finite-size scaling of the condensate fraction (see the SM for details).

With the above bounded range, the precise T_{BKT} can be further extracted from standard finite-size scaling. The most commonly used method is via the data collapse of the pairing correlator $\langle\Delta^2\rangle$ [33,34,36–41]. It is based on the scaling relation $\langle\Delta^2\rangle L^{\eta_c} = f(x)$ with $x = L\times\exp[-A(T/T_{\mathrm{BKT}} - 1)^{-1/2}]$ slightly above the transition as $T \to T^{+}_{\mathrm{BKT}}$ [30,36,41]. The fitting process determines A, η_c, and T_{BKT}, which then make the plot of $\langle\Delta^2\rangle L^{\eta_c}$ collapse into a universal curve of $f(x)$. Similarly, condensate fraction n_c should also satisfy the above scaling relation since it has the same scaling behavior as $\langle\Delta^2\rangle$. We

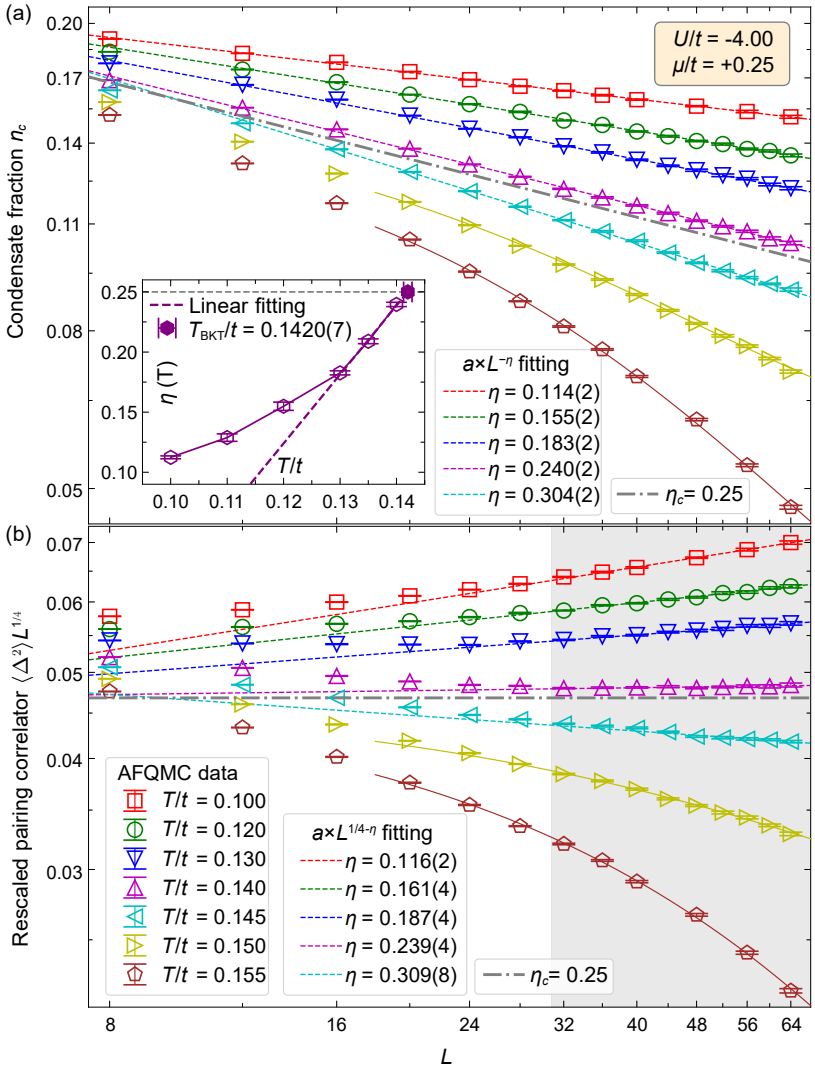

Fig. 1. The finite-size scaling and log-log plots of (a) condensate fraction n_c, and (b) rescaled pairing correlator $\langle\Delta^2\rangle L^{1/4}$, versus linear system size L, for the 2D attractive Fermi-Hubbard model with $U/t = -4, \mu/t = 0.25$. The AFQMC results in both panels share the same legends. The dashed lines represent power-law fits to the data for $L \geqslant 20$ in panel (a), and with $L \geqslant 32$ in panel (b), while the solid lines denote exponential fits. Consistent values of the exponent η are extracted from both quantites for $T/t \leqslant 0.145$. The gray, dash-dot lines highlight $\eta_c = 1/4$ at the BKT transition, with the transition temperature bounded as $0.140 < T_{BKT}/t < 0.145$ [with fermion filling $n \simeq 0.8003$ (see the SM for details)]. The inset in (a) shows a linear extrapolation of η to η_c versus T, yielding a transition temperature $T_{BKT}/t = 0.1420(7)$. The light gray shaded region in (b) marks the scaling regime ($L \geqslant 32$) of $\langle\Delta^2\rangle$, in which it exhibits the correct size-scaling behavior.

then perform data collapse for both n_c and $\langle\Delta^2\rangle$ with fixed $\eta_c = 1/4$ for the results presented in Fig. 1. Considering the finite-size effect in $\langle\Delta^2\rangle$, we use numerical results of $L = 32$–64 for $\langle\Delta^2\rangle$ and $L = 20$–64 for n_c in the fitting, for which we adopt polynomials for $f(x)$ around $x \to 0^+$ and apply the least-squares criterion. The data collapse results are plotted in Fig. 2. Consistent results of $T_{BKT}/t = 0.1413(6)$ and $0.1407(11)$ are obtained respectively from n_c and $\langle\Delta^2\rangle$, which agree with the bounded range obtained in Fig. 1. The insets of Fig. 2, showing relative deviations from $f(x)$ of $L \leqslant 28$ results, reveal the more severe finite-size effect in $\langle\Delta^2\rangle$ than that of n_c. Specifically, the maximum deviation for $L = 20$ is $\sim 10\%$ in $\langle\Delta^2\rangle$, whereas it is $\sim 3\%$ for n_c. Further including $L \leqslant 28$ data in the fitting for $\langle\Delta^2\rangle$ indeed leads to a lower T_{BKT} out of the bounded range.

An alternative way to compute BKT transition temperature is to first obtain the finite-size result $T_{BKT}(L)$ and then extrapolate it to TDL. They satisfy a logarithmic correction relation as $T_{BKT}(L) = T_{BKT}(L = \infty) + a/(\ln bL)^2$ [23–25,30–32]. This method has been applied in numerical simulations of Ising model [31], XY model [25,30], and dipolar boson system [24].

The change from algebraic to exponential scaling behaviors of condensate fraction across the BKT transition naturally gives rise to an inflection point in its temperature dependence, $n_c(T)$. Here we identify this inflection point as $T_{BKT}(L)$. As illustrated in Fig. 3(a) for two representative sets of AFQMC data, we first perform fitting for $n_c(T)$ and then determine the inflection point as the peak location of $-\mathrm{d}n_c/\mathrm{d}T$ using the fitting curve. The uncertainty of $T_{BKT}(L)$ is estimated via bootstrapping [74]. The consistent results of $-\mathrm{d}n_c/\mathrm{d}T$ from the fitting and the numerical differentiation using total-variation regularization [75,76] in the inset of Fig. 3(a) validates our procedure of computing $T_{BKT}(L)$. We repeat this procedure for $L = 8$–64, and perform the scaling for $T_{BKT}(L)$ using the above logarithmic relation. Due to limited precision, we fix the parameter $b = 1$ in the fitting, as in previous studies [24,31,32]. The results for $[U/t = -4, \mu/t = 0.25]$ and $[U/t = -6, \mu/t = 0.50]$ are plotted in Fig. 3(b). TDL transition temperatures of $T_{BKT}(L = \infty)/t = 0.1418(40)$ and $0.1426(41)$ are reached for these two cases, respectively, with $n \simeq 0.8003$ and $n \simeq 0.5766$ at the transition (see the SM for details). These numbers are consistent with those obtained from the $\eta(T)$ scaling and the data collapse [see Figs. 1(a) and 2(a) for $U/t = -4$, and the SM for $U/t = -6$]. The inset of Fig. 3(b) shows the $c + a/(\ln bL)^2$ fitting for $T_{BKT}(L)$, which yields noticeably noisier estimates of $T_{BKT}(L = \infty)$ compared to the fixed $b = 1$ case, but remains consistent within the

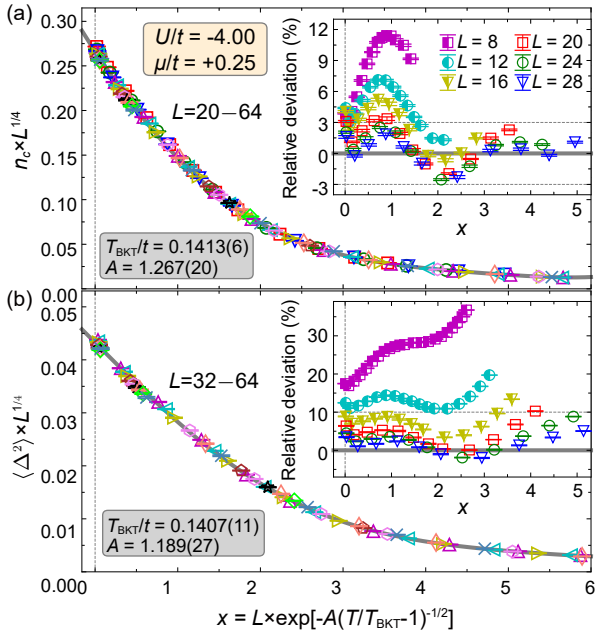

Fig. 2. Data collapse for (a) condensate fraction n_c, and (b) on-site pairing correlator $\langle\Delta^2\rangle$ with fixed exponent $\eta_c = 1/4$. The fitting process involves AFQMC data of $L = 20$–64 for n_c and $L = 32$–64 for $\langle\Delta^2\rangle$, respectively. The gray solid lines are the scaling invariant function $f(x)$, for which we adopt polynomials in x for the fitting. The two insets sharing the same legends plot the relative deviations from $f(x)$ for $L \leqslant 28$ results. Simulation parameters are the same as Fig. 1.

uncertainty. We have also tried polynomial fits in $1/L$ for $T_{\mathrm{BKT}}(L)$, which all produce $T_{\mathrm{BKT}}(L=\infty)$ higher than the corresponding bounded range. It thereby supports the validity of the logarithmic correction form instead.

Highly accurate BKT transition temperature can have broad applications in uncovering the underlying physics of 2D correlated systems. One example is the behavior of thermodynamics near the BKT transition. Among these, specific heat is a particularly important and widely used observable for detecting phase transitions [52]. However, previous studies showed that the specific heat exhibits a peak at $\sim 1.6T_{\mathrm{BKT}}$ in 2D ^{4}He [7] and $\sim 1.17T_{\mathrm{BKT}}$ in 2D XY model [26–30]. Our results also confirm the existence of such anomaly in the 2D attractive Hubbard model. We compute the specific heat using $C_v = (\mathrm{d}E/\mathrm{d}T)/N_s$ with $E = \langle\hat{H}\rangle$ as the total energy. Through fitting E/N_s, the energy derivative is evaluated analytically from the fitting curve. Results of E/N_s ($L = 12$, and $L = \infty$ from extrapolations) and C_v (at TDL) are presented in Fig. 4 for $U/t = -4, \mu/t = 0.25$. The specific heat C_v obtained consistently from both energy fitting and numerical differentiation [75,76] exhibits a pronounced peak at $T_{\mathrm{SpH}} \sim 1.10T_{\mathrm{BKT}}$. Similar behavior is observed in calculations at other fixed values of μ/t, with comparable ratios of $T_{\mathrm{SpH}}/T_{\mathrm{BKT}}$ and a notable trend of decreasing peak height in C_v with reduced filling (see the SM for details). This specific heat anomaly is attributed to the maximal rate of vortex formation which costs energy, as revealed in 2D XY model [26–28], and is therefore not directly related to the BKT transition. Nevertheless, it may serve as a precursor signature of approaching BKT transition in future optical lattice experiments for the 2D attractive Hubbard model, for which the BKT physics remains inaccessible [73].

We have uncovered the scaling behaviors of condensate fraction and developed schemes based on this quantity to estimate BKT transition temperature in the 2D attractive Fermi-Hubbard model. These behaviors and approaches can be readily extended to other 2D correlated fermion systems that exhibit superconductivity or superfluidity, including bilayer models [77–81], systems with spin-orbit coupling (SOC) [62,74,82], and interacting Fermi gases [43,61]. In the presence of SOC, condensate fraction can be similarly computed from a

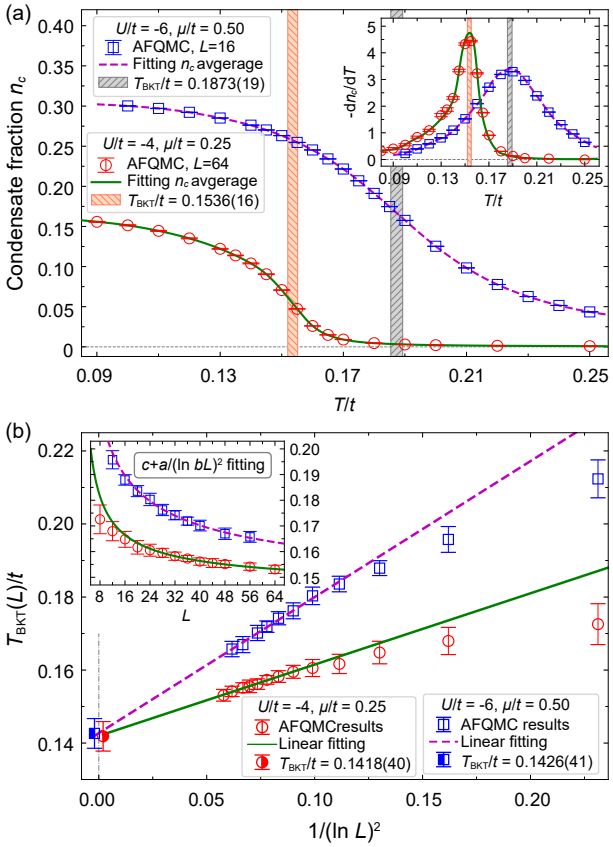

Fig. 3. Finite-size BKT transition temperature $T_{\mathrm{BKT}}(L)$ and its logarithmic correction scaling for the 2D attractive Fermi-Hubbard model. Panel (a) illustrates the determination of $T_{\mathrm{BKT}}(L)$ as the inflection point of condensate fraction $n_c(T)$ curve. A cubic-spline fit is first applied to $n_c(T)$, and $T_{\mathrm{BKT}}(L)$ is identified as the peak position of $-\mathrm{d}n_c/\mathrm{d}T$, with error bars estimated via bootstrapping [74]. The inset plots $-\mathrm{d}n_c/\mathrm{d}T$, with symbols as results from numerical differentiation [75–76]. Panel (b) shows the scaling of $T_{\mathrm{BKT}}(L)$ using $T_{\mathrm{BKT}}(L) = T_{\mathrm{BKT}}(L=\infty) + a/(\ln L)^2$, and the results of $T_{\mathrm{BKT}}(L=\infty)/t$ are also included. The inset plots the fitting of $T_{\mathrm{BKT}}(L)$ using a more compact formula of $c + a/(\ln bL)^2$.

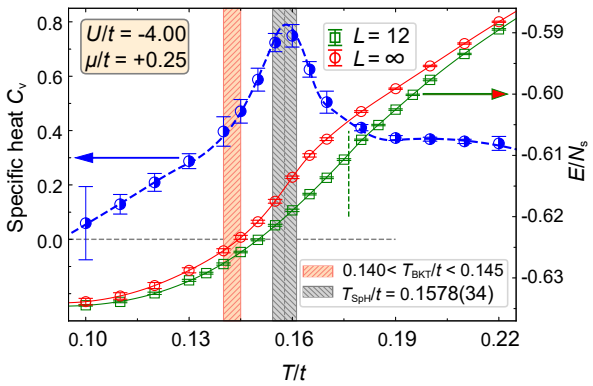

Fig. 4. Specific heat C_v and total energy E/N_s versus T/t for $U/t = -4$, $\mu/t = 0.25$. Energy results of $L = 12$ (green squares) and $L = \infty$ (red circles) with solid lines as polynomial fittings are plotted. TDL results for C_v from the fitting curve of $L = \infty$ energies (blue dash line) and numerical differentiation [75–76] (blue circles) are shown. The peak location of $\mathrm{d}(E/N_s)/\mathrm{d}T$ for $L = 12$ is marked by vertical green dash line as a comparison. The bounded range of T_{BKT}/t and the peak location of specific heat T_{SpH}/t (with the error bar estimated via bootstrapping [74]) are indicated by the shading bands, leading to the anomaly as $T_{\mathrm{SpH}}/T_{\mathrm{BKT}} \sim 1.10$.

modified pairing matrix $M_{kk'}$, which incorporates both spin-singlet and spin-triplet pairing [74,83]. Accordingly, the pairing correlators

suffer the same issues as shown in Fig. 1(b) and the accompanying text, while the logarithmic scaling of $T_{\rm BKT}(L)$ derived from condensate fraction proves to be an efficient way to obtain $T_{\rm BKT}$ at TDL [74]. In a 2D Fermi gas, the dilute limit $n \to 0$ renders the pairing correlator and superfluid density to exhibit vanishing signals, even in the finite system simulations. As a result, condensate fraction becomes the most reliable observable for extracting the transition temperature. To obtain the final $T_{\rm BKT}$ (in unit of Fermi temperature $T_{\rm F}$), a two-step extrapolation procedure for $T_{\rm BKT}(L,N_{\rm e})$ sequentially towards $L \to \infty$ and $N_{\rm e} \to \infty$ is required. As shown in our previous work [43], $T_{\rm BKT}(L,N_{\rm e})$ exhibits a linear dependence on $1/L^2$ at fixed $N_{\rm e}$, while the extrapolated value $T_{\rm BKT}(L=\infty,N_{\rm e})$ follows a logarithmic scaling with $N_{\rm e}$.

Our findings should also be applicable to 2D bosonic systems hosting a superfluid phase, inlcuding the Bose–Hubbard model [84], thin film of ^{4}He [85], and dipolar boson system [24]. In such systems, the condensate fraction can be extracted from the single-particle density matrix $\rho(r) = \langle b_{\mathbf{0}}^{+} b_r \rangle$ [46,86], which can be easily calculated in various many-body numerical approaches. Thus, our proposed schemes of computing $T_{\rm BKT}$ via condensate fraction provide at least competitive alternatives to the widely used method based on the superfluid density [24,85] for many-boson systems.

Conclusion

In summary, we have demonstrated that the condensate fraction captures the essential physics of BKT transition, exhibiting algebraic and exponential size scalings below and above the the transition, respectively. It also allows to determine the transition temperature with several efficient schemes. Our discoveries can be applied to the 2D superconducting and superfluid transitions in a broad class of correlated fermion and boson systems. In the 2D attractive Fermi-Hubbard model, our results show that the condensate fraction scaling exhibits remarkably smaller finite-size effect than the commonly used on-site pairing correlator, and thus can substantially change the prospect of computing BKT transition temperature. We further extract the finite-size transition temperature from the condensate fraction in the model, and confirm its expected logarithmic scaling behavior. Additionally, we compute the specific heat and observe its anomaly in this fermionic system, which may offer valuable guidance for optical lattice experiments aiming to probe BKT transition in attractive fermion systems.

Acknowledgements

The author thanks Youjin Deng, Massimo Boninsegni, and Shiwei Zhang for insightful discussions on the finite-size scaling and applications to bosonic systems. This work was supported by the National Natural Science Foundation of China (Grant Nos. 12247103 and 12204377), the Quantum Science and Technology-National Science and Technology Major Project (Grant No. 2021ZD0301900), and the Youth Innovation Team of Shaanxi Universities.

References

[1] Berezinsky V L 1972 *Sov. Phys. JETP* **34** 610
[2] Kosterlitz J M and Thouless D J 1973 *J. Phys. C: Solid State Phys.* **6** 1181
[3] Kosterlitz J M 1974 *J. Phys. C: Solid State Phys.* **7** 1046
[4] Ryzhov V N, Tareyeva E E, Fomin Y D, and Tsiok E N 2017 *Phys. Usp.* **60** 857
[5] Nelson D R and Kosterlitz J M 1977 *Phys. Rev. Lett.* **39** 1201
[6] Bishop D J and Reppy J D 1978 *Phys. Rev. Lett.* **40** 1727
[7] Ceperley D M and Pollock E L 1989 *Phys. Rev. B* **39** 2084
[8] Beasley M R, Mooij J E, and Orlando T P 1979 *Phys. Rev. Lett.* **42** 1165
[9] Hebard A F and Fiory A T 1980 *Phys. Rev. Lett.* **44** 291
[10] Wolf S A, Gubser D U, Fuller W W, Garland J C, and Newrock R S 1981 *Phys. Rev. Lett.* **47** 1071
[11] Hadzibabic Z, Krüger P, Cheneau M, Battelier B, and Dalibard J 2006 *Nature* **441** 1118
[12] Cladé P, Ryu C, Ramanathan A, Helmerson K, and Phillips W D 2009 *Phys. Rev. Lett.* **102** 170401
[13] Choi J y, Seo S W, and Shin Y i 2013 *Phys. Rev. Lett.* **110** 175302
[14] Ries M G, Wenz A N, Zürn G, Bayha L, Boettcher I, Kedar D, Murthy P A, Neidig M, Lompe T, and Jochim S 2015 *Phys. Rev. Lett.* **114** 230401
[15] Murthy P A, Boettcher I, Bayha L, Holzmann M, Kedar D, Neidig M, Ries M G, Wenz A N, Zürn G, and Jochim S 2015 *Phys. Rev. Lett.* **115** 010401
[16] Sunami S, Singh V P, Garrick D, Beregi A, Barker A J, Luksch K, Bentine E, Mathey L, and Foot C J 2022 *Phys. Rev. Lett.* **128** 250402
[17] Bohlen M, Sobirey L, Luick N, Biss H, Enss T, Lompe T, and Moritz H 2020 *Phys. Rev. Lett.* **124** 240403
[18] Sobirey L, Luick N, Bohlen M, Biss H, Moritz H, and Lompe T 2021 *Science* **372** 844
[19] Christodoulou P, Gałka M, Dogra N, Lopes R, Schmitt J, and Hadzibabic Z 2021 *Nature* **954** 191
[20] Sobirey L, Biss H, Luick N, Bohlen M, Moritz H, and Lompe T 2022 *Phys. Rev. Lett.* **129** 083601
[21] Arisue H 2009 *Phys. Rev. E* **79** 011107
[22] Chatelain C 2014 *J. Stat. Mech.* **2014** P11022
[23] Ueda A and Oshikawa M 2021 *Phys. Rev. B* **104** 165132
[24] Filinov A, Prokof'ev N V, and Bonitz M 2010 *Phys. Rev. Lett.* **105** 070401
[25] Tomita Y and Okabe Y 2002 *Phys. Rev. B* **65** 184405
[26] Tobochnik J and Chester G V 1979 *Phys. Rev. B* **20** 3761
[27] Ota S, Ota S B, and Fahnle M 1992 *J. Phys.: Condens. Matter* **4** 5411
[28] Ota S B and Ota S 1995 *Phys. Lett. A* **206** 133
[29] Gupta R and Baillie C F 1992 *Phys. Rev. B* **45** 2883
[30] Nguyen P H and Boninsegni M 2021 *Appl. Sci.* **11** 4931
[31] Su W Y, Hu F, Cheng C, and Ma N 2023 *Phys. Rev. B* **108** 134422
[32] Sandvik A W 2010 *AIP Conf. Proc.* **1297** 135
[33] Scalettar R T, Loh E Y, Gubernatis J E, Moreo A, White S R, Scalapino D J, Sugar R L, and Dagotto E 1989 *Phys. Rev. Lett.* **62** 1407
[34] Moreo A and Scalapino D J 1991 *Phys. Rev. Lett.* **66** 946
[35] Singer J M, Pedersen M H, Schneider T, Beck H, and Matuttis H G 1996 *Phys. Rev. B* **54** 1286
[36] Paiva T, dos Santos R R, Scalettar R T, and Denteneer P J H 2004 *Phys. Rev. B* **69** 184501
[37] Nakano T and Kuroki K 2006 *Phys. Rev. B* **74** 174502
[38] Paiva T, Scalettar R, Randeria M, and Trivedi N 2010 *Phys. Rev. Lett.* **104** 066406
[39] Fontenele R A, Costa N C, dos Santos R R, and Paiva T 2022 *Phys. Rev. B* **105** 184502
[40] Zhu X, Han W, Feng S, and Guo H 2023 *Phys. Rev. Res.* **5** 023037
[41] Wang X C and Qi Y 2023 *Phys. Rev. B* **107** 224502
[42] He Y Y, Shi H, and Zhang S 2019 *Phys. Rev. Lett.* **123** 136402
[43] He Y Y, Shi H, and Zhang S 2022 *Phys. Rev. Lett.* **129** 076403
[44] Scalapino D J, White S R, and Zhang S C 1992 *Phys. Rev. Lett.* **68** 2830
[45] Scalapino D J, White S R, and Zhang S 1993 *Phys. Rev. B* **47** 7995
[46] Yang C N 1962 *Rev. Mod. Phys.* **34** 694
[47] Astrakharchik G E, Boronat J, Casulleras J, and Giorgini S 2005 *Phys. Rev. Lett.* **95** 230405
[48] Fukushima N, Ohashi Y, Taylor E, and Griffin A 2007 *Phys. Rev. A* **75** 033609
[49] Sears V F and Svensson E C 1979 *Phys. Rev. Lett.* **43** 2009
[50] Zwierlein M W, Stan C A, Schunck C H, Raupach S M F, Kerman A J, and Ketterle W 2004 *Phys. Rev. Lett.* **92** 120403
[51] Inada Y, Horikoshi M, Nakajima S, Kuwata-Gonokami M, Ueda M, and Mukaiyama T 2008 *Phys. Rev. Lett.* **101** 180406
[52] Ku M J H, Sommer A T, Cheuk L W, and Zwierlein M W 2012 *Science* **335** 563
[53] Giorgini S, Pitaevskii L P, and Stringari S 1996 *Phys. Rev. A* **54** R4633
[54] Salasnich L, Manini N, and Parola A 2005 *Phys. Rev. A* **72** 023621
[55] Dell'Anna L, Mazzarella G, and Salasnich L 2011 *Phys. Rev. A* **84** 033633
[56] He R, Li N, Lu B N, and Lee D 2020 *Phys. Rev. A* **101** 063615
[57] Jensen S, Gilbreth C N, and Alhassid Y 2020 *Phys. Rev. Lett.* **124** 090604
[58] Richie-Halford A, Drut J E, and Bulgac A 2020 *Phys. Rev. Lett.* **125** 060403
[59] de Koning M, Cai W, Cazorla C, and Boronat J 2023 *Phys. Rev. Lett.*

130 016001
[60] Salasnich L 2007 *Phys. Rev. A* **76** 015601
[61] Shi H, Chiesa S, and Zhang S 2015 *Phys. Rev. A* **92** 033603
[62] Shi H, Rosenberg P, Chiesa S, and Zhang S 2016 *Phys. Rev. Lett.* **117** 040401
[63] Yang C N 1989 *Phys. Rev. Lett.* **63** 2144
[64] Mark D K and Motrunich O I 2020 *Phys. Rev. B* **102** 075132
[65] Hille C, Kugler F B, Eckhardt C J, He Y Y, Kauch A, Honerkamp C, Toschi A, and Andergassen S 2020 *Phys. Rev. Res.* **2** 033372
[66] Blankenbecler R, Scalapino D J, and Sugar R L 1981 *Phys. Rev. D* **24** 2278
[67] Hirsch J E 1983 *Phys. Rev. B* **28** 4059
[68] White S R, Scalapino D J, Sugar R L, Loh E Y, Gubernatis J E, and Scalettar R T 1989 *Phys. Rev. B* **40** 506
[69] Scalettar R T, Noack R M, and Singh R R P 1991 *Phys. Rev. B* **44** 10502
[70] McDaniel T, D'Azevedo E F, Li Y W, Wong K, and Kent P R C 2017 *J. Chem. Phys.* **147** 174107
[71] He Y Y, Qin M, Shi H, Lu Z Y, and Zhang S 2019 *Phys. Rev. B* **99** 045108
[72] Song Y F, Deng Y, and He Y Y 2025 *Phys. Rev. B* **111** 035123
[73] Hartke T, Oreg B, Turnbaugh C, Jia N, and Zwierlein M 2023 *Science* **381** 82
[74] Song Y F, Deng Y, and He Y Y 2024 *Phys. Rev. B* **109** 094504
[75] Chartrand R 2011 *International Scholarly Research Notices* **2011** 164564
[76] Wietek A, He Y Y, White S R, Georges A, and Stoudenmire E M 2021 *Phys. Rev. X* **11** 031007
[77] Zujev A, Scalettar R T, Batrouni G G, and Sengupta P 2014 *New J. Phys.* **16** 013004
[78] Fontenele R A, Costa N C, Paiva T, and dos Santos R R 2024 *Phys. Rev. A* **110** 053315
[79] Prasad Y, Medhi A, and Shenoy V B 2014 *Phys. Rev. A* **89** 043605
[80] Prasad Y 2022 *Phys. Rev. B* **106** 184506
[81] Prasad Y and Lee H 2024 *Phys. Rev. B* **109** 064506
[82] Rosenberg P, Shi H, and Zhang S 2017 *Phys. Rev. Lett.* **119** 265301
[83] The seperated condensate fractions of singlet and triplet channels can be also extracted, and they can further elucidate their respective contributions to the overall mixed-parity pairing, see Ref. [62,74].
[84] Ohgoe T, Suzuki T, and Kawashima N 2012 *Phys. Rev. B* **86** 054520
[85] Boninsegni M, Prokof'ev N, and Svistunov B 2006 *Phys. Rev. Lett.* **96** 070601
[86] Ceperley D M 1995 *Rev. Mod. Phys.* **67** 279